Journal of Structural Chemistry. Vol. 60, No. 1, pp. 136-142, 2019.

CHARACTERIZATION AND COMPUTATIONAL STUDIES OF 2-(BENZAMIDO)THIAZOL-5-YL BENZOATE

F. Odame[1], E. Hosten[1], R. Betz[1], K. Lobb[2], and Z. Tshentu[1]

2-(Benzamido)thiazolylbenzoate is synthesized via a novel method. It is characterized by spectroscopy, micranalysis, and GC–MS. It crystallizes in the monoclinic space group $P21/n$ with $a = 19.8990(5)$, $b = 7.3680(2)$, $c = 22.3845(6)$ Å, $\beta = 113.799(1)°$, $V = 3002.85(14)$ Å^3, $Z = 8$. The HOMO–LUMO of the reactants and products are considered.

DOI: 10.1134/S0022476619010190

Keywords: synthesis, thiazole, benzoyl chloride, HOMO–LUMO, frontier orbitals.

INTRODUCTION

Thiazoles have shown a broad range of biological activities and are found in many potent biologically active molecules such as Sulfathiazol (antimicrobial drug), Ritonavir (antiretroviral drug), Abafungin (antifungal drug), and Tiazofurin (antineoplastic drug) [1]. They have exhibited some degree of plant growth regulatory and antifungal activities [2], whilst some thiazoles have shown anti-infective [3] as well as antibacterial activities [4]. The regio-controlled synthesis of 2,5-disubstituted and 2,4,5-trisubstituted thiazoles from ethyl-2-bromo-5-chloro-4-thiazolecarboxylates using sequential palladium-catalyzed coupling reactions has been reported [5]. An efficient general method for the preparation of 2,4-di- and trisubsituted thiazoles is via P–TsOH. H_2O-Catalyzed cyclization of trisubstituted propargylic alcohols with thioamides has been accomplished with moderate to excellent product yields under mild and standard conditions [6]. In the presence of triethylamine, (*Z*)-(2-acetoxyl-1-alkenyl) phenyl-λ^3 iodanes reacts with thioureas or thioamides in methanol to afford 2,4-disubstituted thiazoles in good yields. The reaction is thought to proceed by the generation of highly reactive α-λ^3 iodanyl ketones through ester exchange of the β-acetoxy group with liberation of methyl acetate, followed by nucleophilic substitutions with thioureas or thioamides [7]. The resolution of (R)- and (S)-2-(1-hydroxyalkyl) thiazoles (S) in high enantiomeric purity has been reported to be due to a transesterification reaction of the (R) enantiomer with 2,2,2-trifluoroethyl butanoate (TFEB) in diisopropyl ether under immobilized lipase PS catalysis [8]. Ketones have been reacted with NBS in the presence of a catalytic amount of *p*-toluenesulfonic acid to give α-bromoketones in good yields in typical ionic liquids, such as [bmim]PF_6 and [bmpy]Tf_2N, with the ionic liquids being reusable. The one-pot conversion of ketones into thiazoles by treatment with NBS, and subsequently with thioamides has also been carried out in [bmim]PF_6 and [bmpy]Tf_2N, respectively [9]. A thiazole derivative has been accessed by the reaction between 5-chlorothiazol-2-amine and

[1]Department of Chemistry, Nelson Mandela Metropolitan University, Port Elizabeth, South Africa; felixessah15@gmail.com. [2]Department of Chemistry, Rhodes University, Grahamstown, South Africa. *Zhurnal Strukturnoi Khimii*, Vol. 60, No. 1, pp. 143-149, January, 2019. Original article submitted August 29, 2017; revised December 22, 2017; accepted January 04, 2018.

 0022-4766/19/6001-0136 © 2019 by Pleiades Publishing, Ltd.

2,4-difluorobenzoyl chloride in pyridine with stirring [10]. The preparation of 2,4-di- and trisubstituted thiazoles has been achieved *via* *p*-TsOH and $3H_2O$-catalyzed cyclization of trisubstituted propargylic alcohols with thioamides [11]. *N*,*N*-disubstituted β-amino acids and their derivatives with thiazole, aromatic, and heterocyclic substituents have been synthesized from *N*-phenyl-*N*-thiocarbamoyl-β-alanine by the Hantzsch method [12]. The one-pot ring synthesis of novel 4-hydrazinothiazoles has been reported to be accessed by base-assisted eliminative aromatization in the [4+1] ring synthesis; hydrazone deprotection is affected by acylation [13]. Palladium-catalyzed selective olefination of thiazoles has been reported [14]. In this work we report a new method for the synthesis of thiazole and an attempt is made to predict the reactivity from the HOMO–LUMO of the reactants and products.

EXPERIMENTAL

Reagents and instrumentation. Analytical grade reagents and solvents for the synthesis, such as ammonium thiocyanate and glycine, were obtained from Sigma Aldrich (USA) whilst acetone, pyridine, dichloromethane, and benzoyl chloride were obtained from Merck Chemicals (SA). The chemicals were used as received (i.e. without further purification). ^{1}H and ^{13}C NMR spectra were recorded on a Bruker Avance AV 400 MHz spectrometer operating at 400 MHz for ^{1}H and 100 MHz for ^{13}C NMR using DMSO-d_6 as a solvent and tetramethylsilane as the internal standard. Chemical shifts are expressed in ppm. FT–IR spectra were recorded on a Bruker Platinum ATR Spectrophotometer Tensor 27. Elemental analyses were performed using Vario Elementar Microcube ELIII. Melting points were obtained using Stuart Lasec SMP30 whilst the masses were determined using an Agilent 7890A GC system connected to 5975C VL–MSC with electron impact as the ionization mode and detection by a triple-axis detector. GC was fitted with a 30 m × 0.25 mm × 0.25 μm DB-5 capillary column. Helium was used as the carrier gas at a flow rate of 1.6 ml/min with an average rate of 30.2 cm/s and a pressure of 63.7 KPa.

Synthesis of compound I. Ammonium thiocyanate (0.10 mol, 7.6 g) was dissolved in 100 ml of acetone. Benzoyl chloride (0.10 mol, 11.3 ml) was added followed by heating under reflux at 100-120 °C for 2 h. The product was filtered and glycine (0.10 mol, 7.50 g) was added to the filtrate and heated under reflux at 100-120 °C for 6 h. 20 ml of water was then added and the mixture was heated under reflux for further 2 h. The reaction mixture was extracted with diethyl ether, and the solvent was removed *via* rotary evaporation followed by drying the compound under a high vacuum. GC-Mass spectra were recorded for the synthesized compounds and they showed molecular ion (M^+) peaks, in addition to the others, which confirmed the formation of the products. The product recrystallized as a yellow solid from DMSO:toluene (4:1). Yield = 76%, Mp = 198-200 °C. IR (ν_{max}, cm^{-1}): 3227 (N–H), 1704 (C=S), 1665 (C=O), 1520 (C=C), 1406 (C=N). ^{1}H NMR (ppm): 11.50 (s, 1H), 11.15 (s, 1H), 7.95 (d, 2H, Ar–H)), 7.64 (m, 1H, Ar–H), 7.62 (d, 2H, Ar–H), 4.32 (s, 1H, N–H). ^{13}C NMR (ppm): 180.6 (C=S), 169.7 (C=O), 168.1 (C=O), 133.1 (Ar–H), 132.1 (Ar–H) 128.5 (Ar–H), 128.4 (Ar–H) 46.6 (CH_2). LRMS (*m*/*z*, M^+): Found for $C_{10}H_{10}N_2O_3S$ = 312.90, expected mass = 312.41. Anal.calcd. for $C_{10}H_{10}N_2O_3S$: C 50.41, H 4.23, N 11.76, S 13.46. Found: C 50.85, H 4.23, N 11.86, S 13.66.

Synthesis of compound II. Compound **I** (3.24 g, 0.01 mol) was dissolved in acetone (10 ml) and benzoyl chloride (1.40 g, 1.160 ml, 0.01 mol). Pyridine (3 ml) was added slowly over 30 minutes with stirring; the reaction was heated at 80 °C for further two and half h. The solvent was removed at the pump and the product was washed with ethanol to obtain a light purple solid. The product was recrystallized as a light purple solid from THF. Yield = 53%, Mp = 180-182 °C. IR (ν_{max}, cm^{-1}): 3031 (N–H), 3058 (N–H), 1726 (C–S) 1693 (C=O), 1661 (C=O), 1600 (C=C), 1316 (C=N). ^{1}H NMR (ppm): 12.59 (s, 1H, N–H), 8.16 (m, 2H, Ar–H), 8.08 (m, 2H, Ar–H), 7.79 (m, 1H, Ar–H), 7.64 (m, 3H, Ar–H), 7.56 (m, 3H, Ar–H). ^{13}C NMR (ppm): 162.8 (C=O), 134.6 (Ar–H), 130.0 (Ar–H), 129.1 (Ar–H), 128.6 (Ar–H), 128.1 (Ar–H), 127.3 (Ar–H), LRMS (*m*/*z*, M^+): Found for $C_{17}H_{12}N_2O_3S$ = 324.90, expected mass = 324.35. Anal.calcd. for $C_{17}H_{12}N_2O_3S$: C 62.95, H 3.73, N 8.64, S 9.89. Found: C 62.76, H 3.84, N 8.75, S 9.68.

X-ray crystallography. The X-ray diffraction analysis of compound **II** was performed at 200 K using a Bruker Kappa Apex II diffractometer with monochromated MoK_α radiation (λ = 0.71073 Å). APEXII [15] was used for the data

collection and SAINT [15] for the cell refinement and data reduction. The structures were solved by direct methods using SHELXS-2013 [15] and refined by least-squares procedures using SHELXL-2013 [16] with SHELXLE [17] as a graphical interface. All non-hydrogen atoms were refined anisotropically. Carbon-bound H atoms were placed in calculated positions (C–H 0.95 Å for aromatic carbon atoms and C–H 0.99 Å for methylene groups) and were included in the refinement in the riding model approximation, with U_{iso} (H) set to $1.2U_{eq}$ (C). The H atoms of the methyl groups were allowed to rotate with a fixed angle around the C–C bond to best fit the experimental electron density (HFIX 137 in the SHELX program suite [16]), with U_{iso} (H) set to $1.5U_{eq}$ (C). Nitrogen-bound H atoms were located in a difference Fourier map and refined freely. Data were corrected for absorption effects using the numerical method implemented in SADABS [17].

Computational studies. The calculations were carried out using the Gaussian 09 program. Molecular geometries of the singlet ground state of all the compounds were fully optimised in the gas phase at the density functional theory (DFT) level of theory using the hybrid B3LYP functional together with the 6-31G(*d*) basis set. For each compound a frequency calculation was carried out to ensure that the optimized molecular structure corresponded to a minimum, thus only positive frequencies were expected. The HOMO and LUMO results were viewed in Avogadro.

RESULTS AND DISCUSSION

Synthesis and characterization. The ^{1}H NMR spectrum of compound **I** showed a singlet signal at 11.50 ppm for the proton of the hydroxyl group, and another singlet signal at 11.15 ppm was observed for N–H of the amino acid. Isothiocyanate N–H occurred at 4.32 ppm as a singlet signal. A doublet for two protons was observed at 7.95 ppm, while another doublet for two protons occurred at 7.62 ppm. A multiplet for one proton was observed at 7.64 ppm. In the ^{13}C NMR spectrum the thione carbon atom was observed at 180.6 ppm, and those of the acid carbonyl and benzoyl groups occurred at 169.7 ppm and 168.1 ppm respectively. Aromatic carbon atoms were observed between 133.1 ppm and 128.4 ppm. A methylene carbon atom was observed at 46.6 ppm. This was also confirmed in the DEPT-135 spectrum. The IR spectrum showed a signal at 3227 cm^{-1} for the N–H stretching. A signal was observed at 1704 cm^{-1} for the C=S stretching, whilst a signal at 1665 cm^{-1} was observed for the carbonyl group. A signal for the aromatic C=C stretching was observed at 1520 ppm. The ^{1}H NMR spectrum of compound **II** showed a singlet signal at 12.59 ppm for a proton, a multiplet for two protons was observed at 8.16 ppm, another multiplet for two protons was observed at 8.08 ppm, whilst a multiplet signal for a proton was observed at 7.79 ppm. Still the aromatic region a multiplet signal for three protons was observed at 7.64 ppm, whilst another multiplet signal for three protons occurred at 7.56 ppm. The ^{13}C NMR spectrum of compound **II** gave a signal at 162.8 ppm for the carbonyl group; signals between 134.0 ppm and 127.3 ppm were observed for aromatic carbon atoms. The IR spectrum gave signals for N–H at 3031 cm^{-1} and 3058 cm^{-1}, the C–S signal was observed at 1726 cm^{-1}, the carbonyl C=O stretchings were observed at 1693 cm^{-1} and 1661 cm^{-1}, whilst aromatic C=C was observed at 1600 cm^{-1}.

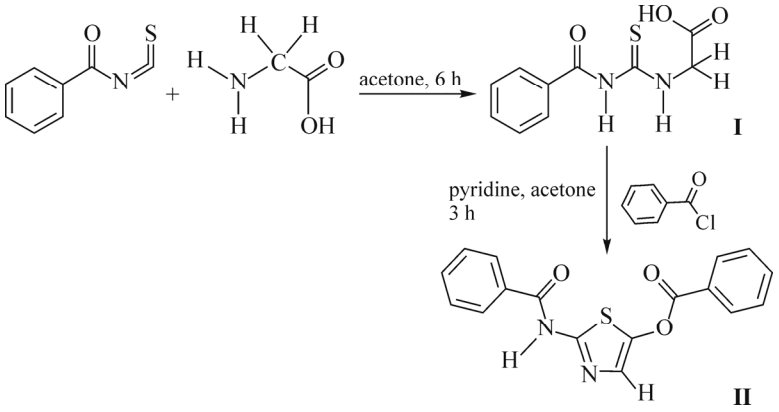

Scheme 1. Synthesis scheme for compounds **I** and **II**.

The reaction is proposed to proceed by the carbonyl attack of benzoyl chloride by the oxygen lone pair of the hydroxyl group, as indicated in **2a** with the loss of hydrochloric acid. Pyridine abstracts a proton from the secondary amine, as indicated in **2b**; the subsequent formation of the C=N double bond led to the migration of electrons from the C=S bond onto the sulfur atom, which allows it to easily attack the carbonyl group from carboxylic acid. The electrons from the C=O bond then move onto the oxygen atom which picks up the abstracted proton from pyridine to form a hydroxyl group in **2c**. Further abstraction of a proton from the methylene group led to the loss of water from **2c**, leading to the formation of the final product (**II**).

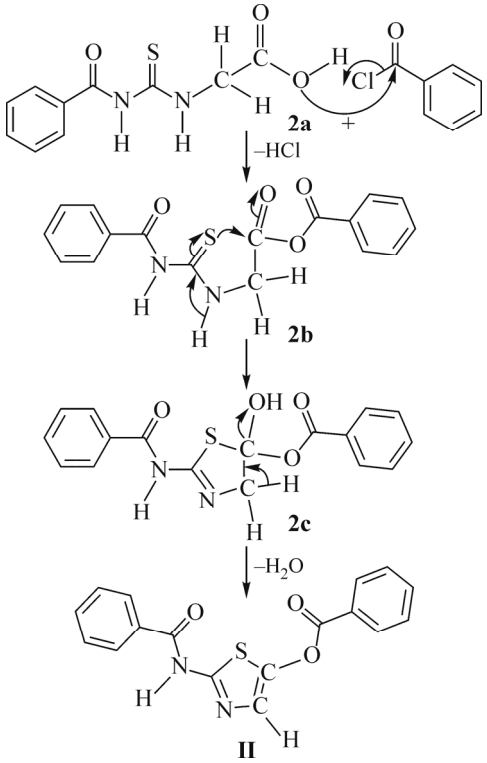

Scheme 2. Proposed mechanism for the synthesis of compound **II**.

X-ray crystallography. The X-ray crystal structure of compound **II** was obtained using single crystals grown by crystallization from THF. Table 1 shows the crystallographic and structure refinement data for compound **II**. It recrystallizes in the monoclinic space group *P*21/*n*. The crystal structure of **II** is formed by two crystallographically independent molecules, one of which is shown in Fig. 1. The S1–C12 and S2–C22 bond distances of 1.737(2) Å and 1.732(2) Å respectively were consistent with the thione (C=S) bond distance. Whilst the C11–O11 and C15–O13 bond distances for the carbonyl groups in **II** were 1.24(2) Å and 1.25(2) Å, respectively (Fig. 1). The N11–C12 and N12–C13 bond distances were 1.384(1) Å and 1.381(2) Å, respectively. The C12–S1–C14 and C22–S2–C24 bond angles of 86.8(1)° and 87.1(1)° were consistent with the bond angle of a thiazole sulfur atom.

Fig. 1 gives the ORTEP view of compound **II** with 50% ellipsoids. In the crystal packing the molecules form dimers through an intermolecular N–H…N H-bond with parameters detailed in Table 2 and Fig. 2. Fig. 2 gives a dimer of compound **II**, which is held together by a hydrogen bond between the amide hydrogen atom and the thiazole nitrogen atom. This is also replicated in another molecule of the dimer.

HOMO–LUMO analysis. Some theoretical studies to characterise the nature of these compounds in terms of the chemical reactivity have been carried out in order to predict the reactivity of these compounds. The HOMO and LUMO and their energy gaps have been evaluated by DFT. The HOMO and LUMO are the main orbitals that determine the chemical

TABLE 1. Crystallographic Data and Structure Refinement Summary for Compound **II**

Property	Compound **II**
Formula	$C_{17}H_{12}N_2O_3S$
CCDC number	1055089
Formula weight	324.35
Crystal system	Monoclinic
Space group	*P*21/*n*
a, *b*, *c*, Å; β, deg.	19.8990(5), 7.3680(2), 22.3845(6); 113.799(1)
V, Å^3	3002.85(14)
Z	8
D(calc), g/cm^3	1.435
μ(MoK_α), mm	0.232
F(000)	1344
Crystal size, mm	0.12×0.24×0.33
Temperature, K	200
Radiation, Å	0.71073
θ_{min}–θ_{max}, deg.	2.0-28.3
Dataset	–26:26; –9:9; –29:29
Tot., uniq. data, *R*(int)	42220, 7477, 0.024
Observed data [$I > 2.0\sigma(I)$]	5898
N_{ref} / N_{par}	7477 / 423
R / wR_2	0.0353 / 0.1003
S	1.02
Max. and av. Shift/error	0.00 and 0.00
Min. / max. residual. dens., e/Å^3	–0.20 / 0.32

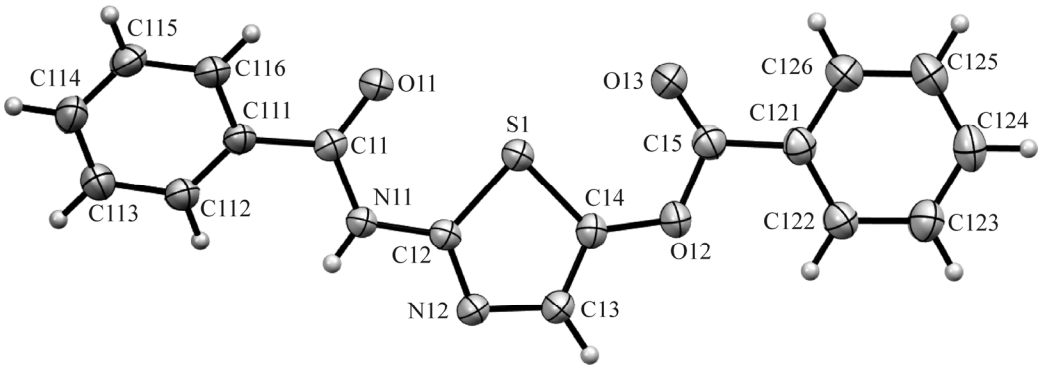

Fig. 1. ORTEP view of compound **II** showing 50% probability displacement ellipsoids and atom labelling.

stability of any species [18]. The HOMO represents the ability to donate an electron whilst the LUMO represent the ability to accept an electron. The LUMO is concentrated on benzoyl chloride when the two reacting species were computed together for their frontier orbitals. Also the HOMO LUMO gap is lower for the two reacting species together (270.17 kJ/mol) than that for compound **I** alone, indicating that the reactivity of compound **I** (391.86 kJ/mol) is improved by the presence of benzoyl chloride due to the susceptibility of benzoyl chloride to attack. The HOMO energy is directly related to the ionization potential whilst the LUMO energy is related to the electron affinity. The HOMO and LUMO energy difference known as the energy gap determines the stability or reactivity of molecules [19]. The energy gap is a critical parameter in determining molecular electrical transport properties because it is a measure of the electron conductivity [20]. The hardness of a molecule

TABLE 2. Parameters of the Intermolecular N–H…N H-Bond

Donor–H…Acceptor	D–H, Å	H…A, Å	D…A, Å	D–H…A, deg.
N11–H11…N22	0.83(2)	2.14(2)	2.947(2)	167.8(15)
N21–H21…N12	0.83(2)	2.14(2)	2.954(2)	169.1(15)

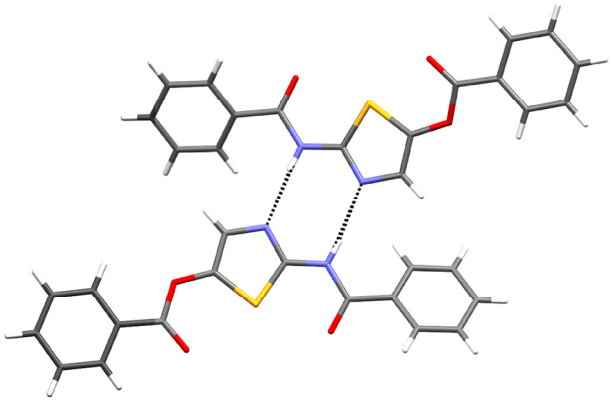

Fig. 2. Dimer of compound **II** showing the H-bonding between the molecules.

TABLE 3. Summary of the HOMO–LUMO Energies for the Reacting Species and Compound **II**

Parameter	HOMO, kJ/mol	LUMO, kJ/mol	HOMO–LUMO Gap, kJ/mol
Benzoyl chloride	–723.06	–203.29	519.77
Reacting species	–523.24	–253.07	270.17
Compound **I**	–539.44	–147.58	391.86
Compound **II**	–570.55	–156.98	413.57

also corresponds to the HOMO–LUMO gap [21]. A large HOMO–LUMO gap indicates a high stability and resistance to charge transfer; therefore, hard molecules have a large HOMO–LUMO gap.

Table 3 gives the computed LUMO and HOMO energy gap of the reacting species and compound **II**. The LUMO of the reacting species shows the delocalization of its orbitals over the benzoyl chloride molecule whilst the HOMO is delocalised over amide, thione, and carboxylic acid in compound **I**. The attack of benzoyl chloride is supposed to be critical for the reaction to happen. In compound **II** the LUMO is delocalized over the entire molecule, indicating that the entire molecule is involved in charge transfer to stabilize the compound.

CONCLUSIONS

2-(Benzamido)thiazolylbenzoate has been synthesized and characterized by spectroscopy, micranalysis, and GC–MS. Its crystal structure has been discussed as well as the HOMO and LUMO of the reactants and the products.

REFERENCES

1. N. Siddiqui, M. F. Arshad, W. Ahsan, and M.S. Alam. *Int. J. Pharm. Sci. Drug. Res*., **2009**, *1*(3), 136-143.
2. H. Yu, L. Shao, and J. Fang. *J. Organomet. Chem*., **2007**, *692*, 991-996.
3. F. P. Bruno, M. R. Caira, E. C. Martin, G. A. Monti, and N. R. Sperandeo. *J. Mol. Struc*., **2013**, *1036*, 318-325.
4. K. Liaras, A. Geronikaki, J. Glamočlija, A. Ćirić, and M. Soković. *Bio. & Med. Chem*., **2011**, *19*, 3135-3140.

5. K. J. Hodgetts and T. M. Kershaw. *Org. Lett*., **2002**, *8*, 1363-1365.
6. M. Ochiai, Y. Nishi, S. Hashimoto, Y. Tscuhimoto, and D. W. Chen. *J. Org. Chem*., **2003**, *68*, 7887/7888.
7. P. Allevi, P. Ciuffreda, G. Tarcco, and M. Anastasia. *J. Org. Chem*., **1996**, *61*, 4144-4147.
8. G. D. Williams and R. A. Pike. *Org. Lett*., **2003**, *22*, 4227**-**4230
9. Y. Izumisawa and H. Togo. *Green Sustainable Chem*., **2011**, *1*, 54-62.
10. X. W. Liu, J. Y. Li, H. Zhang, Y. J. Yang, and J. Y. Zhang. *Acta Crystallogr. E*, **2012**, *68*, o1857.
11. X. Zhang, W. T. Teo, S. H. Chan, and P. W. H. Chan. *J. Org. Chem*., **2010**, *75*, 6290-6293.
12. V. Mickevičius, A. Voskienė, I. Jonuškienė, R. Kolosej, J. Šiugždaitė, P. R. Venskutonis, R. Kazernavičiūtė, Z. Brazienė, and E. Jakienė. *Molecules*, **2013**, *18*, 15000-15018.
13. S. Titus and K. G. Sreejalekshmi. *Tetrahedron. Lett*., **2014**, *55*, 5465-5467.
14. W. Liu, X. Yu, and C. Kuang. *Org. Lett*., **2014**, *16*, 1798-1801.
15. APEX2. SADABS and SAINT. Bruker AXS Inc, Madison, WI, USA, **2010**.
16. G. M. Sheldrick. *Acta Crystallogr. A*, **2008**, *64*, 112-122.
17. C. B. Hübschle, G. M. Sheldrick, and B. Dittrich. *J. Appl. Cryst*., **2011**, *44*, 1281-1284.
18. M. Kurt, P. Chinna Babu, N. Sundaraganesan, M. Cinar, and M. Karabacak. *Spectrochim. Acta A*, **2011**, *79*, 1162-1170.
19. D. F. V. Lewis and C. D. V. Ioannides. *Xenobiotica*, **1994**, *24*, 401-408.
20. L. Padmaja, R. C. Kunar, D. Sajan, I. H. Joe, V. S. Jayakunmar, G. R. Pettit, and O. F. Nielsen. *J. Raman Spectrosc*., **2009**, *40*, 419-428.
21. A. Poiyamozhi, N. Sundaraganesan, M. Karabacak, O. Tanriverdi, and M. Kurt. *J. Mol. Struct*., **2012**, *1024*, 1-12.